A Comparison of Methods for the Registration of Tractographic Fibre Images

Dan Golding*† Marc Tittgemeyer‡ Alfred Anwander§ and Tania Douglas*
*Medical Imaging Research Unit, University of Cape Town, Cape Town, South Africa, Email: dan@golding.za.net
†Advanced Mathematical Modelling Group, Department of Modelling and Digital Science,
Council for Scientific and Industrial Research, Pretoria, South Africa
‡Max Plank Institute for Neurological Science, Cologne, Germany
§Max Plank Institute for Human Cognitive and Brain Science, Leipzig, Germany

***Abstract*—Diffusion tensor imaging (DTI) and tractography have opened up new avenues in neuroscience. As most applications require precise spatial localization of the fibre images, image registration is an important area of research. Registration is usually performed prior to tractography. However more reliable images could be produced if a viable registration can be performed post tractography. This study shows two available techniques for direct registration of fibre images and explores novel adaptations of these. The methods register volume images derived from the fibres, and reapply the transformation from these registrations to the fibre images. The first method is a local affine registration and the second is a global affine registration. The local affine method produced the best results with an average increase in correlation of 0.13 (from 0.34 before registration) per bundle as opposed to an increase of 0.04 for the global method.**

I. Introduction

Diffusion tensor imaging (DTI) and tractography have opened up new avenues in neuroscience and are allowing previously unexplored areas of neuroanatomy and function to be researched. The tractographic fibre images that result from tractography have found applications in, amongst others, surgical planning, reducing postoperative neurological deficit, the development of white matter atlases and the ability to study the relationship between structure and function in the brain by allowing researchers to image connectivity. Most of these applications require precise spatial localization of the images which is achieved through image registration.

The vast majority of research and applications that use tractographic fibre images register the DTI images prior to tractography. DTI registration, which requires voxel re-orientation apart from the normal spatial transformations, is an actively researched and open problem. The fibre tracking process itself accumulates errors along the tracts and thus is sensitive to small changes in the DTI images. Thus registration of the tractographic fibre images rather than the DTI images may produce more accurate and less distorted images than those produced from tractography based on registered DTI images. This study investigates available techniques for direct registration of fibre images and explores novel adaptations of these.

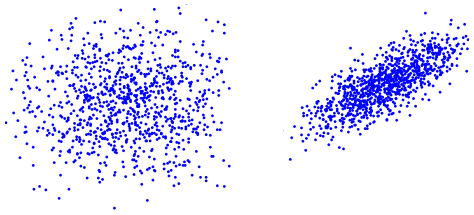

(a) (b)

Fig. 1. Illustrations of (a) isotropic diffusion and (b) anisotropic diffusion.

II. Background

A. Diffusion Tensor Imaging and Tractography

Diffusion tensor imaging (DTI) is a relatively new magnetic resonance imaging (MRI) modality that enhances conventional MRI to image the 3D structure of fibrous tissues [1], [2]. The properties of water diffusion in tissue enable this. Water diffusion, whilst normally isotropic, is slightly inhibited by cell membranes. In tissue made up of long, thin cells, i.e. fibrous tissue, the diffusion of water becomes anisotropic as water diffusion is inhibited across the cells but not along their bodies [3]. Figure 1 illustrates the difference between isotropic and anisotropic diffusion.

Diffusion affects MRI by lowering the signal intensity. Originally considered a source of noise in MRI, diffusion weighted images (DWI) can be created by measuring this loss of signal from at least seven directions. A diffusion tensor can be fit to each voxel of the DWI image to create a DTI. This tensor gives the probability that water will diffuse in any direction from that voxel. DTI images are used as a basis to create a variety of different image types that are simpler to interpret visually. Two common types are fractional anisotropy (FA) maps and deterministic tractographic images. Figure 2 shows these image types.

FA is a measure of anisotropy and is defined as

$$FA = \sqrt{\frac{\left((\lambda_1-\lambda_2)^2+(\lambda_2-\lambda_3)^2+(\lambda_3-\lambda_1)^2\right)}{2\left(\lambda_1^2+\lambda_2^2+\lambda_3^2\right)}} \quad (1)$$

where λ_1, λ_2 and λ_3 are the eigenvalues of the diffusion tensor. Tractography is the process of tracking potential fibre

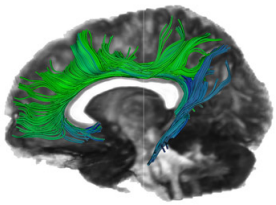

Fig. 2. A deterministic tractographic image of the cingulum superimposed on a FA map showing a sagital section of the brain.

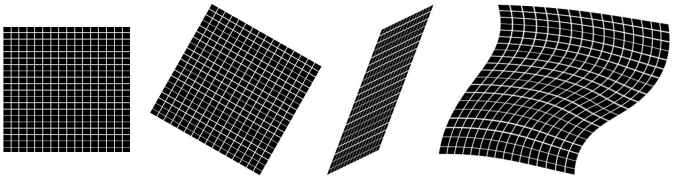

Fig. 3. Examples of different types of transformations applied to a grid. The transformations are: (a) Identity transformation, (b) Rigid 6 DOF transformation, (c) Affine 12 DOF transformation and (d) Nonlinear transformation.

trajectories from the DTI images [4]. As the white matter fibres of the brain follow convoluted trajectories, this type of image is an invaluable aid to the understanding and interpretation of their structure and orientation. Tractographic images fundamentally differ from other MRI images in that they are morphometric [5]. The images are not based on voxels but are rather represented as a group of trajectories, each representing a single fibre. Each fibre is an ordered set of 3D coordinates in continuous space, spaced discretely along the fibre. This is important as conventional image registration algorithms cannot be applied directly to these sorts of images.

B. Image Registration

Registration is the process of transforming an image to be as spatially aligned to a reference image as possible [6]. DTI images are almost always accompanied by images of the same subject but differing in modality such as an FA map, a conventional T2 MRI image or a functional MRI image. Inter-modal registration allows precise spatial localization across these images. Intra-modal registration is also important as it allows spatial localization across multiple subjects.

A registration can be categorized by whether it is inter-modal or intra-modal, inter-subject or intra-subject and also by the type of transformation applied to the input image [7]. The most important transformation for this study is the affine transformation, described by Equation 2, which has 12 degrees of freedom (DOF) in 3D. Figure 3 shows different transformations applied to a simple image.

$$\begin{pmatrix} x' \\ y' \\ z' \\ 1 \end{pmatrix} = \begin{pmatrix} l_{11} & l_{12} & l_{13} & t_x \\ l_{21} & l_{22} & l_{23} & t_y \\ l_{31} & l_{32} & l_{33} & t_z \\ 0 & 0 & 0 & 1 \end{pmatrix} \begin{pmatrix} x \\ y \\ z \\ 1 \end{pmatrix} \qquad (2)$$

where the l_{ij} parameters are the nine parameters of a linear transformation, the t_i parameters are the translations in 3D, x, y, and z are the input coordinates and x', y', and z' are the transformed coordinates.

Registration typically consists of four components: A transformation, an interpolation, a similarity metric and an optimization algorithm. The transformation is applied to an input image to increase its similarity with a reference image. Interpolation is needed to apply transformations to the discreet voxel based images. An optimization algorithm iteratively finds the parameters of the transformation by maximizing the similarity between the transformed image and the reference image [7].

Conventional registration algorithms cannot be applied directly to DTI images as each voxel contains directional information. If the transformation contains a component of rotation, it is important to re-orient the diffusion tensor in each voxel accordingly [8]. For a purely rigid transformation, the rotational component of the transformation can be applied as it is to each of the voxels. Applying an affine transformation to a diffusion tensor would violate an accepted assumption that the transformation should only alter the orientation of the diffusion tensors and not change their size or shape. Thus for affine transformations, simply applying the transformation to each voxel is not satisfactory. Two methods are proposed to account for this. The first is the finite strain method [9], where the rotational component is extracted from the affine transformation via matrix decomposition. The second is the principle diffusion directions method which can account for stretches and shears. The linear portion of the affine matrix is applied to the principle diffusion direction and then normalizes it according to the magnitude of this product [9].

C. The Current State of DTI and Tractographic Image Registration

Although image registration is in widespread use, it is far from an infallible process [10]. These flaws are more prominent in the newer and more complex process of registering DTI images. Tractography itself is not a robust process. As fibre tracking is based on integration, small errors between the DTI voxels are amplified along the fibres, such as the small errors introduced by image registration.

There are remarkably few publications proposing algorithms that register tractographic images directly, i.e. after fibre tracking. One method registers a single fibre bundle as an input image to a whole brain tractography as a reference using affine transformations [11]. Two works have used nonlinear transformations by finding local affine transformations and combining them [12], [13]. However the algorithms are not comprehensively documented and the methods used to validate success are subjective or ambiguous.

III. Methods

Two experiments are contrasted in this study. In both of the experiments the fibre data used are physically meaningful

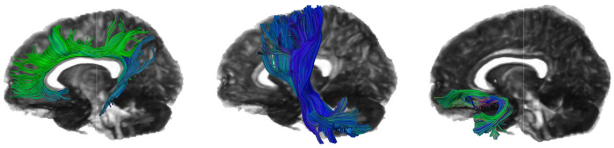

(a) (b) (c)

Fig. 4. Examples of the segmented fibre bundles used showing (a) the cingulum, (b) the corticofugal tract and (c) the uncinate fasciculus.

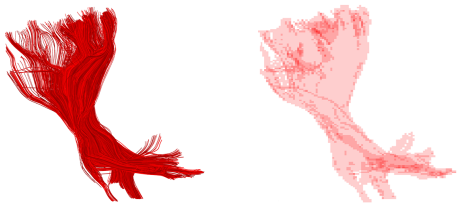

(a) (b)

Fig. 5. A fibre volume (a) and its corresponding binary volume (b).

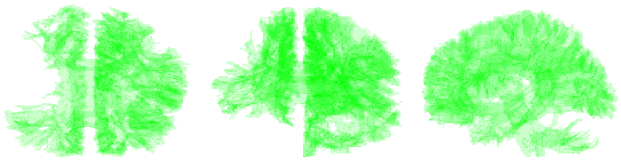

Fig. 6. Example of a binary volume from all the fibre bundles of a brain image from three orthogonal views. The asymmetry is the result of only using fibre bundles in the right hemisphere.

bundles of fibres segmented out of the whole brain tractography. This allows the success of registration on the internal structures of the brain, which exhibit a high variability, to be assessed. Figure 4 shows examples of these segmented fibre bundles. The dataset consists of 10 brain images each with 13 segmented bundles. The bundles are made up of 1300 fibres on average and each fibre consists of 100 3D data points on average. The bundles are from the right side of the brain or the centre. Bundles from the left side are not represented as the brain can be taken as symmetrical and are therefore redundant. The data were supplied by the Max Plank Institute of Human Cognitive and Brain Science in Leipzig, Germany.

A. Local Affine Registration

Registration tools for MRI brain images are widely available. These tools operate on conventional MRI images, FA maps and even DTI images. However there are no tools available that can register fibre data. Instead of recreating a registration algorithm, the fibre images are converted into a form that can be used by existing tools in this study.

Each fibre bundle is converted to a volume. Affine registration is performed directly on these volumes and then reapplied to the source fibre images using equation 4. A separate registration is performed on each fibre bundle, rather than finding on affine transformation for the entire source image. These local affine transformations can later be combined into a single nonlinear transformation for the entire image using a polyaffine framework as done in [13].

Volumes were produced by finding spatial probability density functions (PDF) for each fibre bundle according to the equation [13]:

$$\mathbf{P}_{b_i}(\vec{x}) = \frac{1}{Z} \sum_{t_j \in b_i} \sum_{\vec{x}_k \in t_j} \kappa(\vec{x} - \vec{x}_k) \tag{3}$$

where b_i is a fibre bundle, t_j is a single fibre and $\vec{x}_k$ is a point on a fibre defined as a 3D spatial vector. $\vec{x}$ is the 3D spatial coordinate of the probability distribution, i.e. the voxel coordinate, Z is a normalizing constant chosen to make the values of $\mathbf{P}_{b_i}(\vec{x})$ sum to 1 and $\kappa(\vec{x} - \vec{x}_k)$ is a Gaussian kernel centred around $\vec{x}_k$. The fibre bundles that are used in this project have on average 1300 fibres per bundle with an average of 100 points per fibre. Multiplied by the $160 \times 200 \times 160$ voxels of each DTI image, Equation 3 needs to calculate 0.7 trillion values to create a probability density function (PDF) for one, average fibre bundle. This is very computationally expensive. This study compared the use of such a PDF as the volume against a simple binary volume derived from the fibre bundles. Figure 5 shows an example of such a binary volume.

The affine transformation produced by an affine registration of the volume images is simple to reapply to the fibre images. The transformation assumes that the centre of rotation is the centre of the image and so half of each pixel dimension, represented by the vector $\vec{N}_{1/2}$, must be subtracted from a point before applying the affine transformation and added back afterwards. This processed can be expressed as:

$$\vec{p'} = \mathbf{A}^{-1}(\vec{p} - \vec{N}_{1/2}) + \vec{N}_{1/2} \tag{4}$$

where $\vec{p}$ is the source point, $\vec{p'}$ is the transformed point and $\mathbf{A}$ is the affine matrix or the form shown in equation 2. The matrix is inverted as the output from the registration tool gives the transformation to get back to the source.

B. Global Affine Registration

One single global volume is created for each source image by combining the individual volumes from each fibre bundle. Binary volumes are used as the volume-based local affine experiment showed that they outperform the PDFs and are incomparably faster. These results are given in Section IV. Figure 6 shows an example of such a whole brain binary volume.

C. Validation

The success of each registration was assessed by converting the fibre bundle into a binary volume and calculating 6 similarity metrics between the volume derived from the transformed fibres and the volume derived from the reference fibres. The metrics are:

- The Pearson correlation coefficient given by equation 5
- Four overlap metrics, target overlap, $T_{\mathbf{SR}}$, source overlap, $S_{\mathbf{SR}}$, mutual overlap, $M_{\mathbf{SR}}$, and union overlap, $U_{\mathbf{SR}}$ which are given by equation 6

TABLE I
MEAN OF IMPROVEMENT OF FIBRE REGISTRATIONS PER METHOD.

Method	Cross Correlation	Target Overlap	Source Overlap	Mutual Overlap	Union Overlap	Cohen's Kappa
Local	0.1309	0.11	0.15	0.13	0.10	0.1321
Global	0.0445	0.03	0.06	0.04	0.03	0.0442

- Cohen's Kappa.

where $\vec{x}$ is a vector describing the voxel coordinates and $s_{\vec{x}}$ and $r_{\vec{x}}$ are the intensities of the source image, **S** and the reference image, **R** at voxel $\vec{x}$.

$$R_{\mathbf{SR}} = \frac{n\sum_{\vec{x}} s_{\vec{x}} r_{\vec{x}} - \sum_{\vec{x}} s_{\vec{x}} \sum_{\vec{x}} r_{\vec{x}}}{\sqrt{n\sum_{\vec{x}} s_{\vec{x}}^2 - \left(\sum_{\vec{x}} s_{\vec{x}}\right)^2}\sqrt{n\sum_{\vec{x}} r_{\vec{x}}^2 - \left(\sum_{\vec{x}} r_{\vec{x}}\right)^2}}. \quad (5)$$

$$\begin{aligned} T_{\mathbf{SR}} &= \frac{|\mathbf{S}\cap\mathbf{R}|}{|\mathbf{R}|}, & S_{\mathbf{SR}} &= \frac{|\mathbf{S}\cap\mathbf{R}|}{|\mathbf{S}|}, \\ M_{\mathbf{SR}} &= 2\frac{|\mathbf{S}\cap\mathbf{R}|}{|\mathbf{S}|+|\mathbf{R}|}, & U_{\mathbf{SR}} &= \frac{|\mathbf{S}\cap\mathbf{R}|}{|\mathbf{S}\cup\mathbf{R}|} \end{aligned} \quad (6)$$

Cohen's Kappa is traditionally a statistical measure of repeatability used with categorical data. [14] and [15] describe a method to use Cohen's Kappa to measure the similarity of two fibre bundles. This is done by converting each bundle to a binary volume. Voxels are divided into 4 categories namely those that are empty in both images, the sum of which defines S_{nn}, those that contain a tract in both images whose sum is S_{pp}, those that contain a tract in the source image but not the reference image, S_{np}, and those containing tracts in the reference image but not the source, S_{pn}. The number of voxels expected to be empty is then defined as $E_{nn} = (S_{nn} + S_{np})(S_{nn} + S_{pn})/N$ and the number expected to contain tracts is $E_{pp} = (S_{pp} + S_{np})(S_{pp} + S_{pn})/N$, where N is the total number of voxels in each image. Observed agreement (OA) is $(S_{nn} + S_{pp})/n \times 100$ and expected agreement (EA) is $(E_{nn} + E_{pp})/n \times 100$. Cohen's Kappa is then given as

$$\kappa = \frac{OA - EA}{100 - EA} \quad (7)$$

For consistency, κ will be denoted $K_{\mathbf{SR}}$ in this paper.

IV. RESULTS

Figure 7 shows a single fibre bundle from each of the 10 images used in this experiment superimposed on each other in different colours. This figure illustrates the success or failure of a registration as the success is inversely proportional to the colour separation. It is clear that the local affine registration gave the best results followed by the global affine registration. An example of a visual assessment is provided as Figure 9. Figure 8 shows the mean improvement of each of the methods for each of the similarity metrics.

Figure 10 shows the results of the comparison between binary volumes and PDFs. The binary volumes clearly outperform the PDFs in the image and the average time per bundle was decreased from 32 hours for the PDF to 0.21 seconds for the binary volumes.

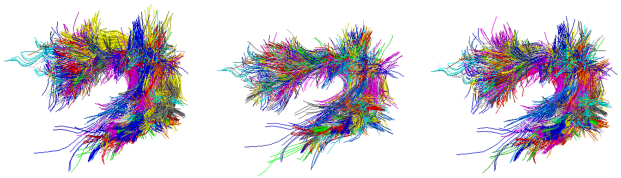

(a) (b) (c)

Fig. 7. Comparison of methods using the volume of the arcuate fasciculus as an example. The bundles from each of the 10 brain images are shown in different colours superimposed on one another. (a) shows the source images, (b) the output images from the local affine registration, and (c) the output images from the global affine registration.

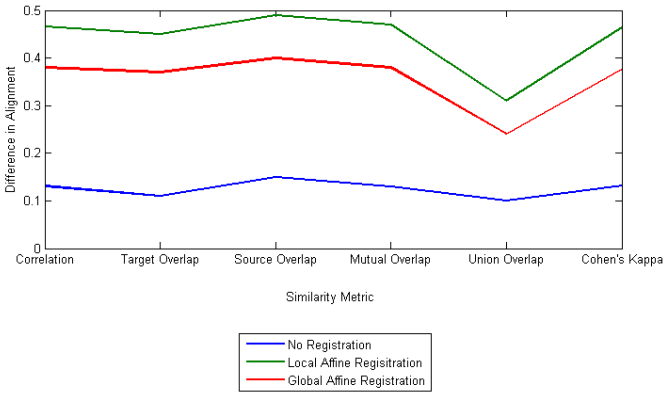

Fig. 8. Mean improvement of fibre registrations per method.

V. DISCUSSION

The experiments show that the direct registration of fibre images produces alignment of individual fibre bundles. The

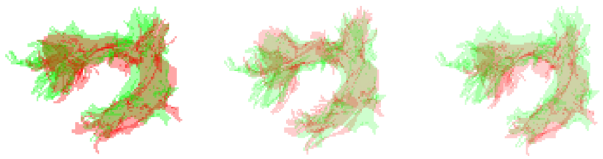

(a) (b) (c)

Fig. 9. Comparison of methods using the volume of the arcuate fasciculus as an example. The green volume is the reference bundle and is identical in all five images. The red volume is: (a) the source image, (b) the output from the local affine registration, and (c) the output from the global affine registration.

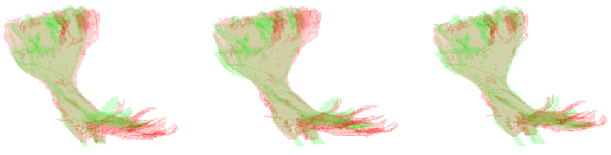

(a) (b) (c)

Fig. 10. Comparison of output volumes from fibre registration using PDF and binary volumes as the base registration. The green volumes are from the reference fibres and the red volumes are from (a) the source fibres, (b) the output fibre from the registration of PDFs and (c) the output fibres from the registration of binary volumes.

tracked fibres will not suffer from the accumulative error introduced by the imperfect spatial realignment and voxel re-orientation of DTI registration as the fibre tracking is performed prior to the registration.

Figure 8 shows that the local affine registration substantially outperforms the global affine method. This is shown visually in Figure 7, where Figure 7(b) is clearly the image with all 10 bundles most closely aligned. Variability in the size, shape and orientation of cortical structures in primates is particularly pronounced [16]. This ratifies the observation that a better alignment can be found by aligning corresponding structures separately rather than aligning the entire brain image globally.

The six metrics for measuring the alignment of the fibre bundles generally agree. The values for Cohen's Kappa all fall in the *moderate agreement* category as defined by [17]. Cohen's Kappa is usually used as a measure of inter-rater agreement and has been used to measure alignment of fibre bundles for intra-subject, rigid transformations.

The use of binary volumes as a base registration over PDFs in the local-affine registration proved not only to be faster but also to produce registrations of a higher quality. It takes almost 70000 times longer to calculate the PDF volume of a fibre bundle as it does to find the equivalent binary volume.

VI. Conclusion

DTI and tractography have produced new images that are allowing the intricate structure of the white matter fibres in the brain to be studied for the first time. Precise localization across images is essential and is achieved through image registration. Registration of DTI images is complicated by the fact that each voxel needs to be re-oriented aside from the spatial reorganization of the voxels. This process is still an open problem. Tractography is an error prone process which is not robust to changes in the DTI image. It is reasonable to assume that tractography prior to the registration of the DTI image will produce more accurate results than tracking fibres after registration. The problem of registering tractographic images has had very little attention in the literature. This project compared two methods of registering fibre images directly. The first method found local affine transformations for each bundle by converting the bundles to binary volumes. The binary volumes are faster to calculate and produce superior results to PDFs as used in the literature. This method is the most successful improving the correlation by 0.13, more than twice the improvement of the global method. The local affine method is superior due to the high variability in the cortical structures of humans, which a global affine transformation cannot account for.

Acknowledgment

Dan Golding received a studentship from the CSIR for his MSc studies in Biomedical Engineering, and further funding was provided by the University of Cape Town and the NRF.

References

[1] P. J. Basser, J. Mattiello, and D. LeBihan, "Estimation of the effective self-diffusion tensor from the NMR spin echo," *Journal of magnetic resonance. Series B*, vol. 103, no. 3, pp. 247–254, 1994.

[2] P. Basser and C. Pierpaoli, "Microstructural and physiological features of tissues elucidated by quantitative-diffusion-tensor MRI," *Journal of Magnetic Resonance-Series B*, vol. 111, no. 3, pp. 209–219, 1996.

[3] C. Beaulieu, "The basis of anisotropic water diffusion in the nervous system - a technical review." *NMR in biomedicine*, vol. 15, no. 7-8, pp. 435–55, 2002.

[4] P. Basser, S. Pajevic, C. Pierpaoli, J. Duda, and A. Aldroubi, "In vivo fiber tractography using DT-MRI data," *Magnetic Resonance in Medicine*, vol. 44, no. 4, pp. 625–632, 2000.

[5] S. Mori, *Introduction to diffusion tensor imaging*. Elsevier Science Ltd, 2007.

[6] D. L. Hill, P. G. Batchelor, M. Holden, and D. J. Hawkes, "Medical image registration." *Physics in medicine and biology*, vol. 46, no. 3, pp. R1–45, Mar. 2001.

[7] J. Maintz and M. a. Viergever, "A survey of medical image registration," *Medical Image Analysis*, vol. 2, no. 1, pp. 1–36, Mar. 1998.

[8] D. Alexander, J. Gee, and R. Bajcsy, "Strategies for data reorientation during non-rigid warps of diffusion tensor images," in *Medical Image Computing and Computer-Assisted Intervention–MICCAI 99*. Springer, 1999, pp. 463–472.

[9] D. Alexander, C. Pierpaoli, P. Basser, and J. Gee, "Spatial transformations of diffusion tensor magnetic resonance images," *IEEE Transactions on Medical Imaging*, vol. 20, no. 11, pp. 1131–1139, 2002.

[10] G. Rohde, "Registration Methods for Quantitative Imaging," PhD Dissertation, University of Maryland, 2005.

[11] A. Mayer and H. Greenspan, "Bundles of interest based registration of white matter tractographies," *2008 5th IEEE International Symposium on Biomedical Imaging: From Nano to Macro*, pp. 919–922, May 2008.

[12] R. Shadmi, A. Mayer, N. Sochen, and H. Greenspan, "Piecewise smooth affine registration of point-sets with application to DT-MRI brain fiber-data," *2010 IEEE International Symposium on Biomedical Imaging: From Nano to Macro*, pp. 528–531, 2010.

[13] U. Ziyan, M. Sabuncu, L. O'Donnell, and C. Westin, "Nonlinear registration of diffusion MR images based on fiber bundles," in *Proceedings of the 10th international conference on Medical image computing and computer-assisted intervention-Volume Part I*. Springer-Verlag, 2007, pp. 351–358.

[14] S. Wakana, A. Caprihan, M. Panzenboeck, J. Fallon, M. Perry, R. Gollub, K. Hua, J. Zhang, H. Jiang, P. Dubey, and Others, "Reproducibility of quantitative tractography methods applied to cerebral white matter," *Neuroimage*, vol. 36, no. 3, pp. 630–644, 2007.

[15] A. N. Voineskos, L. J. O. Donnell, N. J. Lobaugh, D. Markant, S. H. Ameis, M. Niethammer, B. H. Mulsant, B. G. Pollock, J. L. Kennedy, C.-F. Westin, and M. E. Shenton, "NeuroImage Quantitative examination of a novel clustering method using magnetic resonance diffusion tensor tractography," *NeuroImage*, vol. 45, no. 2, pp. 370–376, 2009.

[16] J. Bjaalie, "Localization in the brain: new solutions emerging," *Nature reviews neuroscience*, vol. 3, no. 4, pp. 322–325, 2002.

[17] J. Landis and G. Koch, "The measurement of observer agreement for categorical data." *Biometrics*, vol. 33, no. 1, p. 159, 1977.